

Ultra-selective flexible add and drop multiplexer using rectangular optical filters based on stimulated Brillouin scattering

Wei Wei,^{1,2} Lilin Yi,^{1,*} Yves Jaouën,² Michel Morvan,³ and Weisheng Hu¹

¹State Key Lab of Advanced Optical Communication Systems and Networks, Shanghai Jiao Tong University, Shanghai 200240, China

²Institut Mines-Télécom, Télécom ParisTech, CNRS UMR 5141, 46 Rue Barrault, 75634 Paris, France

³Institut Mines-Télécom, Télécom Bretagne, CNRS UMR 3192, Technopôle Brest-Iroise, France

*lilinyi@sjtu.edu.cn

Abstract: We demonstrate an ultra-selective flexible reconfigurable add and drop multiplexer (ROADM) structure enabling separation and aggregation operations for multi-band orthogonal frequency division multiplexing (MB-OFDM) signal with ~2-GHz spectral granularity and 300-MHz guard band. The ROADM employs rectangular optical filters based on stimulated Brillouin effect (SBS) in fiber, which have steep edges, ~1-dB passband ripple and tunable bandwidth from 100 MHz to 3 GHz realized by two different kinds of electrical feedback pump control approaches. The ROADM performance is measured with MB-OFDM signals in quadrature-phase-shift-keying (QPSK) and 16-quadrature-amplitude-modulation (16-QAM) formats. For QPSK format signal, the SBS-ROADM induced penalty is ~0.7 dB while the performance for 16-QAM format is also acceptable.

©2015 Optical Society of America

OCIS codes: (060.4265) Networks, wavelength routing; (290.5900) Scattering, stimulated Brillouin.

References

1. A. Lord, P. Wright, and A. Mitra, "Core networks in the flexgrid era," *J. Lightwave Technol.* **33**(5), 1126–1135 (2015).
2. N. Sambo, P. Castoldi, F. Cugini, G. Bottari, and P. Iovanna, "Toward high-rate and flexible optical networks," *IEEE Commun. Mag.* **50**(5), 66–72 (2012).
3. O. Gerstel, M. Jinno, A. Lord, and S. J. B. Yoo, "Elastic optical networking: A new dawn for the optical layer?" *IEEE Commun. Mag.* **50**(2), s12–s20 (2012).
4. D. Rafique, T. Rahman, A. Napoli, S. Calabro, and B. Spinnler, "Technology options for 400 Gb/s PM-16QAM flex-grid network upgrades," *IEEE Photon. Technol. Lett.* **26**(8), 773–776 (2014).
5. M.-F. Huang, A. Tanaka, E. Ip, Y.-K. Huang, D. Qian, Y. Zhang, S. Zhang, P. Ji, I. Djordjevic, T. Wang, Y. Aono, S. Murakami, T. Tajima, T. Xia, and G. Wellbrock, "Terabit/s Nyquist superchannels in high capacity fiber field trials using DP-16QAM and DP-8QAM modulation formats," *J. Lightwave Technol.* **32**(4), 776–782 (2014).
6. E. Pincemin, M. Song, J. Karaki, O. Zia-Chahabi, T. Guilloisou, D. Grot, G. Thouenon, C. Betoule, R. Clavier, A. Poudoulec, M. Van der Keur, Y. Jaouën, R. Le Bidan, T. Le Gall, P. Gravey, M. Morvan, B. Dumas-Feris, M. Moulinard, and G. Froc, "Multi-band OFDM transmission at 100 Gbps with sub-band optical switching," *J. Lightwave Technol.* **32**(12), 2202–2219 (2014).
7. S. Frisken, G. Baxter, D. Abakoumov, H. Zhou, I. Clarke, and S. Poole, "Flexible and grid-less wavelength selective switch using LCOS technology," in *Optical Fiber Communication Conference/National Fiber Optic Engineers Conference 2011, OSA Technical Digest (CD)* (Optical Society of America, 2011), paper OTuM3.
8. R. Rudnick, A. Tolmachev, D. Sinefeld, O. Golani, S. Ben-Ezra, M. Nazarathy, and D. Marom, "Sub-banded/singlesub-carrier drop-demux and flexible spectral shaping with a fine resolution photonic processor," in *Proc. ECOC2014 (Cannes, France)*, paper PD.4.1.
9. X. Zou, M. Li, W. Pan, L. Yan, J. Azaña, and J. Yao, "All-fiber optical filter with an ultranarrow and rectangular spectral response," *Opt. Lett.* **38**(16), 3096–3098 (2013).

10. B. Little, S. Chu, W. Chen, J. Hryniewicz, D. Gill, O. King, F. Johnson, R. Davidson, K. Donovan, W. Chen, and S. Grubb, "Tunable bandwidth microring resonator filters," in Proc. ECOC2008(Brussels, Belgium), paper Th.2.C.2.
11. Y. Qin, J. Sun, M. Du, and J. Liao, "Variable single-passband narrowband optical filter based on forward stimulated interpolarization scattering in photonic crystal fiber," *Opt. Lett.* **37**(17), 3720–3722 (2012).
12. A. Wise, M. Tur, and A. Zadok, "Sharp tunable optical filters based on the polarization attributes of stimulated Brillouin scattering," *Opt. Express* **19**(22), 21945–21955 (2011).
13. Y. Stern, K. Zhong, T. Schneider, R. Zhang, Y. Ben-Ezra, M. Tur, and A. Zadok, "Tunable sharp and highly selective microwave-photonic band-pass filters based on stimulated Brillouin scattering," *Photonics Res.* **2**(4), B18–B25 (2014).
14. L. Yi, W. Wei, Y. Jaouën, and W. Hu, "Ideal rectangular microwave photonic filter with high selectivity based on stimulated Brillouin scattering," in Optical Fiber Communication Conference, OSA Technical Digest (online) (Optical Society of America, 2015), paper Tu3F.5.
15. W. Wei, L. Yi, Y. Jaouën, and W. Hu, "Bandwidth-tunable narrowband rectangular optical filter based on stimulated Brillouin scattering in optical fiber," *Opt. Express* **22**(19), 23249–23260 (2014).
16. W. Wei, L. Yi, Y. Jaouën, M. Morvan, and W. Hu, "Brillouin rectangular optical filter with improved selectivity and noise performance," *Photon. Technol. Lett.* (posted 12May 2015, in press).
17. W. Wei, L. Yi, Y. Jaouën, M. Morvan, and W. Hu, "Ultra-selective flexible add-drop multiplexer using rectangular stimulated Brillouin scattering filters," in Optical Fiber Communication Conference, OSA Technical Digest (online) (Optical Society of America, 2015), paper Tu3D.1.
18. V. Lanticq, S. Jiang, R. Gabet, Y. Jaouën, F. Taillade, G. Moreau, and G. P. Agrawal, "Self-referenced and single-ended method to measure Brillouin gain in monomode optical fibers," *Opt. Lett.* **34**(7), 1018–1020 (2009).
19. N. A. Olsson and J. P. Van Der Ziel, "Characteristics of a semiconductor laser pumped Brillouin amplifier with electronically controlled bandwidth," *J. Lightwave Technol.* **5**(1), 147–153 (1987).
20. E. Awwad, Y. Jaouën, and G. R. Othman, "Polarization-time coding for PDL mitigation in long-haul PolMux OFDM systems," *Opt. Express* **21**(19), 22773–22790 (2013).
21. P. Winzer, A. Gnauck, A. Konczykowska, F. Jorge, and J. Dupuy, "Penalties from in-band crosstalk for advanced optical modulation formats," in 37th European Conference and Exposition on Optical Communications, OSA Technical Digest (CD) (Optical Society of America, 2011), paper Tu.5.B.7.

1. Introduction

With the continuing growth in the amount of traffic, high spectral-efficient modulation formats and reduced channel spacing are required. Flex-grid networking has emerged as a key requirement for future dynamic and more efficient networks [1–3]. In this context, flexible super-channel approaches, such as Nyquistwavelength-division-multiplexing (WDM) and multi-band orthogonal frequency division multiplexing (MB-OFDM) are considered to be promising candidates for 400 Gbps and 1 Tbps long-haul WDM transmission due to their high spectral efficiency, small requisite guard band and all-optical sub-band switching superiority [4–6]. One of the core techniques for the flex-grid networking is the super-channel switching strategy, which is realized in a reconfigurable optical add and drop multiplexer (ROADM). The extraction-aggregation of a sub-band signal from dense WDM channels requires a very high-resolution frequency selectivity and makes flexible narrowband filters the most important component.

An ideal solution for flex-grid ROADM is a rectangular optical filter with precise bandwidth and central wavelength tunability. Such kind of rectangular filters with large bandwidth have already been achieved employing liquid-crystal on silicon (LCoS) [7] and bulk-grating techniques [6], which are widely used in add and drop demonstrations. However, for both techniques, the flat-topped passband shape can only be obtained for bandwidth larger than ~tens of GHz. For small bandwidth such as 10 GHz case, the filter passband tends to a Gaussian shape, which cannot completely meet sub-wavelength switching requirements. Moreover, due to the grating and liquid crystal resolution limitation, it is difficult to realize filters with ~GHz bandwidth using these techniques. Thus it is unfit for supporting ultra-narrow flexible switching. The current state-of-art in small-grid flexible ROADM is based on arrayed-waveguide grating and LCoS technique [8]. It can reach ~0.8 GHz resolution and ~GHz bandwidth. However the in-band filter shape is not flat and shows a slow roll-off, which both induces signal distortions and requires larger guardband. For implementing GHz-bandwidth rectangular filter, several solutions have been proposed

including specially designed fiber Bragg gratings (FBG) [9], cascaded micro-ring resonators [10], forward stimulated interpolarization scattering [11] and stimulated Brillouin scattering (SBS) [12–14], etc. Among all the above methods, SBS active filter has been considered as a promising technique with inherent flexibility. Based on SBS effect, recently we have demonstrated rectangular optical filters with tunable bandwidth from 50 MHz to 4 GHz [15]. The filter passband ripple is suppressed to ~ 1 dB using precise digital feedback control. The filter selectivity can reach ~ 40 dB with pump-splitting dual-stage scheme [16].

In this paper, we realize an ultra-selective ROADM structure with ~ 2 -GHz spectral granularity and 300-MHz guard band. We propose two different kinds of feedback methods to achieve rectangular SBS filters for ROADM applications. One is based on a sweeping probe signal generated by an electrical vector network analyzer (EVNA) [15], and the other is based on coherent detection directly using OFDM signal as a probe. Both methods obtain desired results and have similar convergence speed. Based on this rectangular filter, we demonstrate the separation and aggregation of a 3-band OFDM signal in quadrature-phase-shift-keying (QPSK) and 16-quadrature-amplitude-modulation (16-QAM) formats. For the “proof of concept”, we limit the demonstration to a single polarization MB-OFDM signal. The bandwidth of each OFDM band is only 2-GHz and the net bit-rate is ~ 5 Gbit/s using 16-QAM modulation format. Thanks to the steep edges of the proposed filter, the guard band can be set to as small as 300-MHz without any obvious extra penalty. Actually the guard band is only limited by the laser drift and can be further decreased. For QPSK format signal, the filter induced total penalty is only ~ 0.7 dB benefiting from the flat passband and smooth phase response. For 16-QAM format signal, the ROADM performance is also acceptable considering the low tolerance of the noise and crosstalk. Some preliminary results have been presented previously [17], in this paper we demonstrate the proposed novel feedback method in detail including the convergence speed comparison and we further investigate the influence of the Brillouin gain on the ROADM performance.

2. The rectangular SBS filter generation

In order to realize a flexible and precise add and drop function of a ROADM, we first implement a rectangular optical filter with high flexibility. The filter generation process is shown in Fig. 1. First we use an arbitrary waveform generator (AWG) to generate an electrical comb. Then the electrical comb modulates a continuous-wave (CW) light to generate the optical comb acting as the pump. After boosted to a high power level, the pump gives rise to the SBS effect. If the signal is shifted downward from the pump to the Brillouin frequency, it will be amplified as the Stokes wave, and if it is shifted upward to the Brillouin frequency, it will be absorbed as the anti-Stokes wave [18]. This can also be considered as filtering in terms of signal selection. As shown in Fig. 1, in order to obtain a rectangular gain spectrum using Lorentzian-shape natural SBS gain, a pump consisting of equal-amplitude spectral lines with intervals equaling the natural SBS gain bandwidth is required. The programmable AWG allows of controlling the amplitude and the initial phase of each spectral line in the electrical comb digitally and precisely. This approach brings about many benefits. First, the natural SBS bandwidth is only ~ 20 MHz, thus the filter bandwidth can be very small and the controlling precision is very high. Second, the electrical comb is generated precisely by the AWG within a specific frequency range, ensuring the steep filter edges. Third, the amplitude of each comb line can be altered precisely to optimize the filter passband flatness. Fourth, the number of the comb line can be changed to adjust the filter bandwidth precisely. Fifth, the filter central wavelength can also be shifted by tuning the wavelength of the comb electrically and optically. Thus the proposed filter is almost an ideal rectangular filter with multi-dimensional flexibility. In this section, we focus more on the bandpass filter as an example. Note that the filter can be either bandpass with SBS amplification or band-stop with SBS absorption.

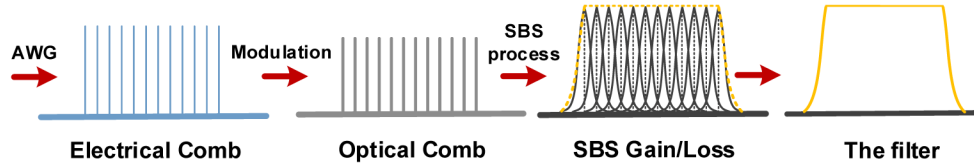


Fig. 1. The principle of the filter generation.

The rectangular optical filter generation has been introduced in our previous publication [15]. Given the nonlinear responses of electrical and optical components, the flat electrical spectral lines actually lead to uneven SBS gain, thus a feedback compensation is proposed to digitally control the amplitude of each electrical spectral line according to the measured SBS gain so as to optimize the shape of the targeted SBS filter. In order to mitigate the incalculable gain induced by four wave mixing (FWM) effect among the multiple pump lines, we set frequency interval of the electrical spectral lines randomly around the natural SBS gain bandwidth instead of the equal interval. In this case the FWM induced gain is no longer superposing on the original lines and the feedback process is more accurate. Note that once the feedback compensation is completed, the optimal pump waveform is fixed and can be stored in the AWG memory for future use. Thus it can be considered as a software-defined optical filter.

At first, we used the whole pump to amplify the signal in a single fiber section. However with the increase of the filter bandwidth, the filter gain cannot be increased effectively by simply increasing the pump power due to both the competition between SBS and Stimulated Raman effect (SRS) and four wave mixing (FWM) induced out-of-band gain. In order to increase the filter selectivity, we propose a pump-splitting dual-stage scheme [16]. Instead of using a single pump with high power, we split it into two stages and amplify the signal twice successively. In this case, the pump power of each stage is under the threshold of the SRS and induce less out-of-band FWM components. Moreover, the decrease in pump power for each stage will decrease the induced noise from the spontaneous Brillouin emission [19]. Thus not only can the filter selectivity be increased dramatically but also better noise performance can be achieved.

The amplitude and phase responses are measured by amplifying an optical sweeping probe signal which is modulated by an electrical sweeping signal from an EVNA. The SBS gain spectrum can be obtained by comparing the results between the SBS pump switched on and off. We reasonably assume that the SBS gain at a certain frequency is only related to the corresponding electrical spectral line. Thus once the SBS gain shape has been obtained, we can use the relation between the SBS gain and the electrical spectral line from the AWG to calculate new amplitude of each electrical spectral line applied to the AWG [15]:

$$\frac{\text{Ideal gain (dB)}}{\text{Measured gain (dB)}} = \left(\frac{\text{Electrical amplitude new}}{\text{Electrical amplitude used}} \right)^2 \quad (1)$$

Since the SBS gain is only related to the pump power which is proportional to the electrical spectral lines, we just set a random phase for each line to maintain an acceptable peak to average ratio of the waveform. More details can be found in Ref [15]. After only 5-10 iterations of the digital feedback compensation, we obtain the long-term stable rectangular filter shape as shown in Fig. 2 with different gain values, in other words, with different filter selectivity. It can be tuned by changing the total pump power. The filter bandwidth can also be tuned by easily changing the number of the electrical spectral lines. The filters with bandwidth from 100 MHz to 3 GHz are illustrated in Fig. 3. The tuning resolution can be as small as ~20 MHz equaling the natural SBS gain bandwidth. No matter what the filter selectivity and bandwidth are, the passband ripple can always be suppressed to ~1 dB and the filter edges are very steep. Due to the flat passband, the filter phase responses are very

smooth. The passband flatness and the smooth phase response can keep signal fidelity to the extreme. The out-of-band gain is due to the FWM components which cannot be mitigated completely. The larger the SBS gain is, the severer the FWM will be.

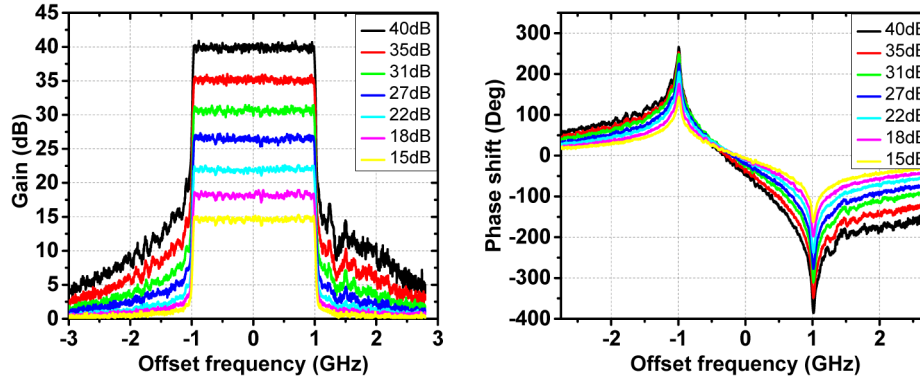


Fig. 2. The (a) amplitude and (b) phase responses of SBS gain filters with tunable selectivity.

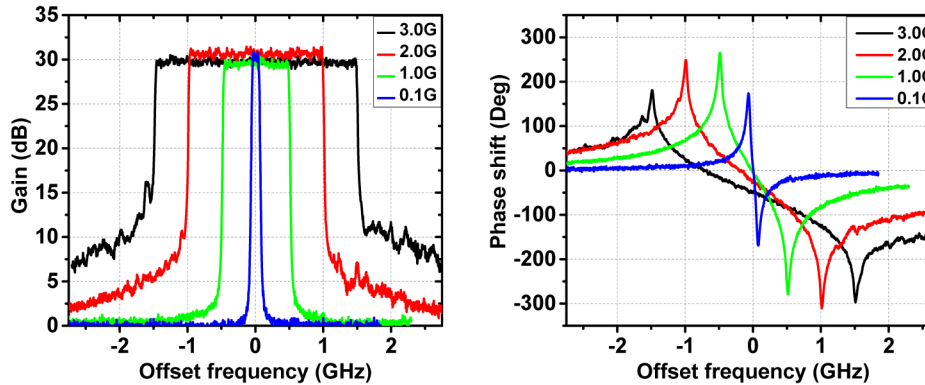


Fig. 3. The (a) amplitude and (b) phase responses of SBS gain filters with tunable bandwidth.

3. Novel feedback method based on the coherent detection

In the previous work, the filter feedback process is based on a sweeping probe generated by an EVNA. This method needs an extra modulator to convert electrical sweeping signal to optical signal, a narrowband filter to suppress one probe sideband and also a photodiode to convert the amplified optical signal back to electrical domain for measurement, which increases the system complexity dramatically. Thus we propose a novel feedback method based on coherent detection. Note that Nyquist-WDM and OFDM signals present flat in-band spectrum thus they can be directly used as the probe signal for the feedback process. Besides, using transmission signal as the probe not only can obtain flat SBS gain, but also can track and compensate the small variation of both channel condition and SBS parameters to ensure stable and optimal filtering state at all times.

The feedback experimental setup is shown in Fig. 4. In the upper branch, an AWG is used to generate the electrical spectral lines with random frequency interval within ± 1 -MHz deviation from the natural SBS bandwidth of 20 MHz, (i.e. 19 MHz, 20 MHz and 21 MHz). Then it modulates a CW light from a distributed feedback (DFB) laser to generate the optical carrier-suppressed single-sideband (OCS-SSB) SBS pump lines utilizing an I&Q modulator (IQM). After being boosted by a high power erbium-doped fiber amplifier (EDFA), the OCS-SSB signal is then split into two parts equally and sent into two identical 25-km long single mode fibers (SMFs), which are under the same strain and temperature conditions to ensure

the same Brillouin characteristics. In each stage, a polarization controller (PC) is used to maintain the SBS gain at the maximum value. It should be noted that a polarization scramblers or a polarization state switch may allow of eliminating the polarization dependent gain (PDG) issue as long as the adjust speed of the scrambler or switch is fast enough where the pump can be treated as being depolarized. In that case, the PCs can be removed from the setup. The SBS gain is ~ 11 -GHz away from the pump as shown in Fig. 4(i). In the lower branch, a QPSK format OFDM signal with constant amplitude from the AWG modulates another CW light by a Mach-Zehnder modulator (MZM) to generate the probe signal as shown in Fig. 4(ii). After passing through an isolator (ISO), the probe OFDM signal propagates in the two fibers successively and the central part within the SBS gain region is amplified twice as shown in Fig. 4(iii) and 4(iv). Finally the amplified OFDM signal is sent into a coherent receiver (which will be described in details in section 4) and the amplitude of each OFDM subcarrier can be obtained after cyclic prefix removal and being transferred to frequency domain using off-line processing. By comparing the amplitude before and after the SBS amplification, the SBS gain spectrum can be obtained. The SBS loss spectrum can also be obtained with the same approach. The feedback process is almost the same with that in the sweeping probe method mentioned in section 2. The only difference is how we obtain the SBS gain spectrum. It should be noted that the OFDM signal used for feedback is different from that used for system performance evaluation in section 4. The bandwidth of the probe OFDM signal is larger than that of SBS filter. Thus the full filter passband and nearby stopband can be detected at the same time. The precision of the gain spectrum obtained by OFDM probe is 20 MHz equaling the interval of OFDM subcarriers which is worse than the spectrum precision obtained by EVNA. However the feedback compensation with current precision can fully meet the system requirement of filter flatness which is proved by the system performance.

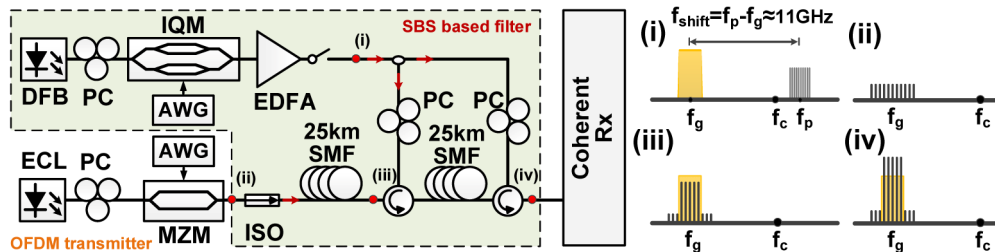


Fig. 4. The dual-stage SBS filter and the feedback process based on coherent detection using OFDM signal. Inset (i) single sideband pump f_p , SBS gain around f_g , and DFB laser frequency f_c , (ii) OFDM signal as a probe with bandwidth larger than pump, (iii) OFDM probe signal amplified by the first stage SBS gain filter, (iv) OFDM probe signal amplified by the second stage SBS gain filter.

Figure 5 illustrates the filter passband shape after proposed feedback compensation with different gains. As shown in the figure, the OFDM-based feedback method obtains similar filter flatness of ~ 1 dB as the sweeping probe approach thus proving its feasibility. However, when the gain increases to ~ 32 dB, the ripple is increased to ~ 2 dB. This does not imply the failure of the feedback. Actually, this is due to the limitation of the receiver dynamic range. In order to ensure the signal with high SBS gain still within the receiver dynamic range, the unamplified original signal should be very small and is easy to fluctuate affected by random noise from the receiver.

The feedback convergence speed of two different methods is shown in Fig. 6. To be fair comparison, we set the same bandwidth of ~ 2.2 GHz and ~ 21 dB gain for both approaches. The figure shows that both approaches have fast and similar convergence speed. Only 5~10 iterations are needed to obtain the flat passband. Theoretically, more iterations lead to flatter filter passband. But the ripple measurement accuracy is limited by the power measurement

precision of the EVNA and coherent detection. Thus there is no practical meaning to pursue very small ripple value. Note that the number of feedback iteration is dependent on the filter bandwidth and gain. The larger the bandwidth and gain, the more iterations are needed to achieve the same flatness level.

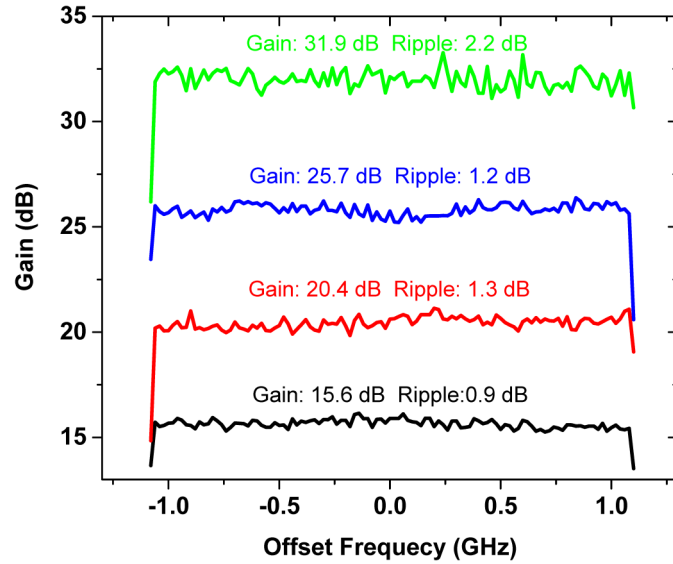


Fig. 5. Filter passband shapes after feedback process based on coherent detection using OFDM signal as the probe. The spectrum precision is ~ 20 MHz equaling the interval of the OFDM subcarriers.

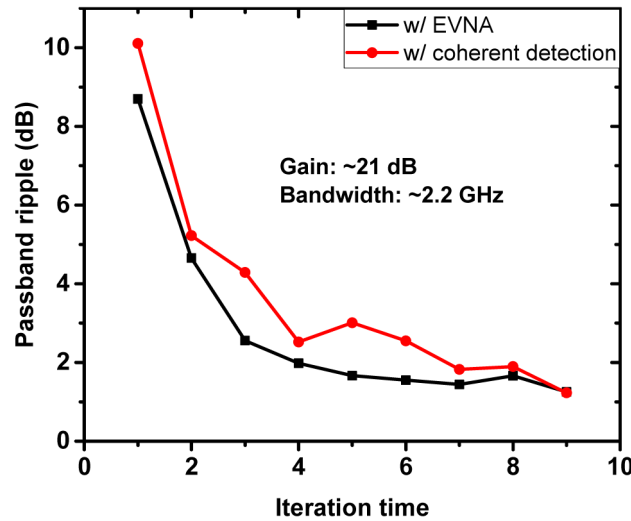


Fig. 6. Typical convergence speed of the two different feedback methods.

4. The ROADM experiment and results

Once the rectangular filters have been obtained, the ultra-selective ROADM can be implemented. The flexible-grid ROADM structure is shown in Fig. 7. An SBS gain filter (bandpass) only keeps the desired band to realize the drop function meanwhile an SBS loss filter (stop-band) removes the band in the MB-OFDM signal to empty the spectral band for another signal to add in. Thanks to the filter central wavelength and bandwidth tunability, the

ROADM can be flexibly configured with very high resolution. Meanwhile the guard band between different bands can be set very small benefiting from the steep edges of the rectangular filter.

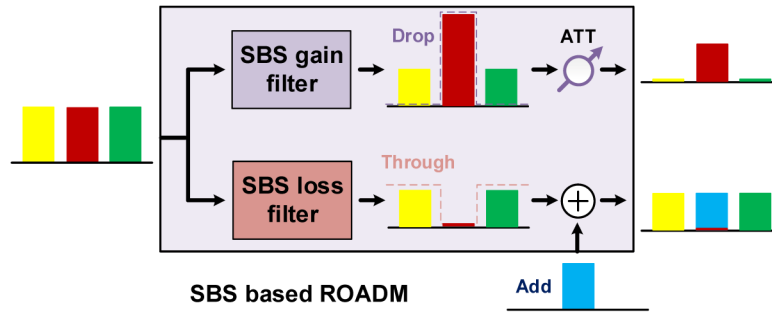


Fig. 7. Concept of the SBS-based ROADM. The SBS gain filter and loss filter are used to realize drop and through function at the same time.

As shown in Fig. 8, the experimental setup consists of three parts: the transmitter, the SBS based ROADM itself and the coherent receiver. In the transmitter part, the light from an external cavity laser (ECL) and 2 DFB lasers operating at ~ 1543 nm are modulated by the electrical OFDM signal. Since we are only interested in the central band signal, we use the same modulator for the two side-band signal generation to reduce the system complexity. As only a single output of the AWG (Tektronix 7221B) is available for OFDM signal generation, an OFDM signal satisfying the Hermitian symmetry is generated. This constraint does not affect our analysis as all subcarriers are treated independently at the receiver side. Given the instability of the 3 lasers, the minimum guard band among the 3 signal bands is set to 300 MHz. For each band, 128 subcarriers are used in order to mitigate phase noise of the ECL with ~ 100 kHz linewidth. Both QPSK and 16-QAM modulation formats have been employed for each subcarrier at the sampling rate of 2.5 GS/s. The bandwidth is set to 2 GHz by adjusting the number of empty subcarriers. After passing through an isolator to block inverse pump light, the single polarization 3-band signal is split into 2 parts. The central band is absorbed or amplified by a 2.2-GHz rectangular dual-stage SBS loss or gain filter in the separate branches respectively. Due to lab constraints, we use 25-km SMF28 for each stage amplification. The extra 200 MHz allows for slight laser drift. After passing through a 12.5-km long fiber, the amplified central band in the upper path is de-correlated with the 2 side bands in the lower path. Then the 3 bands are combined together with the same polarization state adjusted by using 2 PCs. The signal from the ROADM is adjusted to the optimal power and a broadband amplified spontaneous emission (ASE) noise source is added for the bit error rate vs. signal to noise ratio (SNR-BER) measurement. Finally the OFDM signal is detected by a typical coherent receiver. A narrow linewidth ECL laser is used as local oscillator. I and Q parts of the complex optical signal is obtained by using 90-degree hybrids and are then converted to electrical signals with balanced detectors. 50 GS/s real time oscilloscope (Tektronix DPO72004B) digitizes the waveform and generates the sampled digital sequence which is then sent to the computer. QPSK and 16-QAM constellations are then obtained by off-line processing. A more precise description of OFDM signal generation and detection is in [20].

Concerning the SBS pump generation, we use the second AWG output to generate a 2.2-GHz wide electrical signal, which modulates the light from 2 DFB lasers. The amplitude of the electrical comb is well controlled using feedback compensation algorithm described in section 3. An IQM is used to realize OCS-SSB modulation for SBS gain and loss pump generation. After pre-amplification, the 2 pump waves with around 22-GHz frequency spacing are separated by a Finisar waveshaper and boosted to a higher level acting as the

pump. Note that the waveshaper is not required if another IQM is used for gain/loss pump generation. In each stage, a PC is used to maintain the SBS gain or loss at the maximum value through the 25-km long fiber. An EDFA after the first loss filter stage and a variable optical attenuator (VOA) after the second gain filter are used to maintain the 3 bands at the same power level.

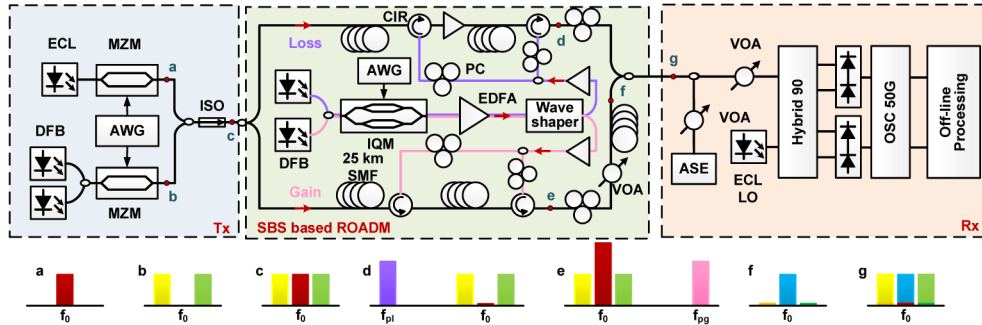


Fig. 8. Experimental setup and the optical spectrum schemes at different points.

The spectra obtained from the oscilloscope are shown in Fig. 9. Due to the low cut-off frequency limitation of the receiver, 12 carriers in the central position are suppressed. Figure 9(b) illustrates the drop function with an SBS gain filter. Only a small parts of the adjacent bands close to the central position are amplified slightly thus making a ~20 dB selectivity. Figure 9(c) illustrates the through function with an SBS loss filter. The central band is completely absorbed and the central peak is only due to the receiver DC noise. After inserting the dropped band to the central empty position shown in Fig. 9(d), the spectrum looks almost the same as the original one shown in Fig. 9(a).

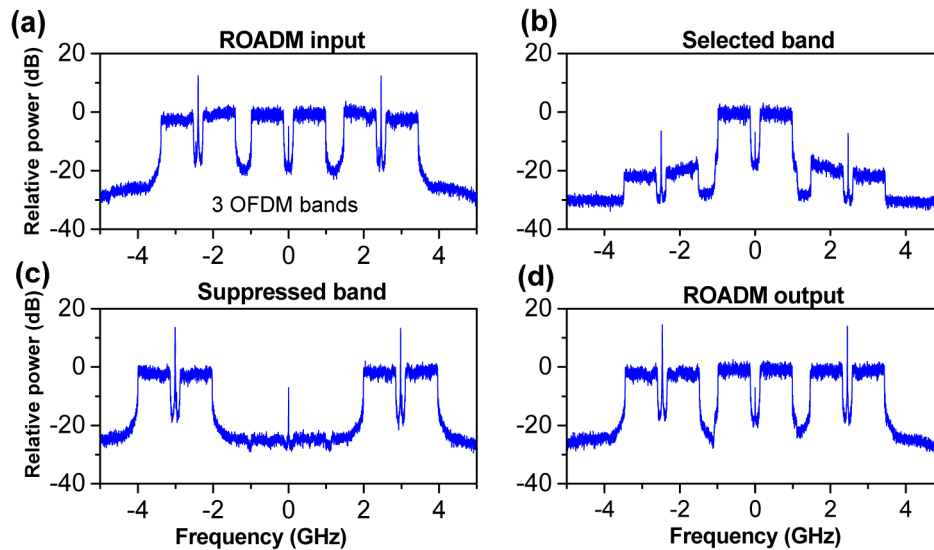


Fig. 9. The electrical spectra of the OFDM signal at different points of the ROADM

In order to further prove the feasibility of the proposed ROADM structure. We evaluate the ROADM performance by BER-SNR measurements. The SNR of the signal is measured in electrical domain as shown in Fig. 10. First we measure the average power level of the whole signal band, which is the total power of the signal and noise. Then we measure the average noise level on the two sides of the signal within the same bandwidth as the signal. Since the

noise is generated from a broad ASE noise, the noise level should be uniform in a wide range and the measured noise on the two sides approximately equals the noise level right in the signal band. After we obtain the estimated noise power and total power of the signal with noise, the SNR can be easily calculated.

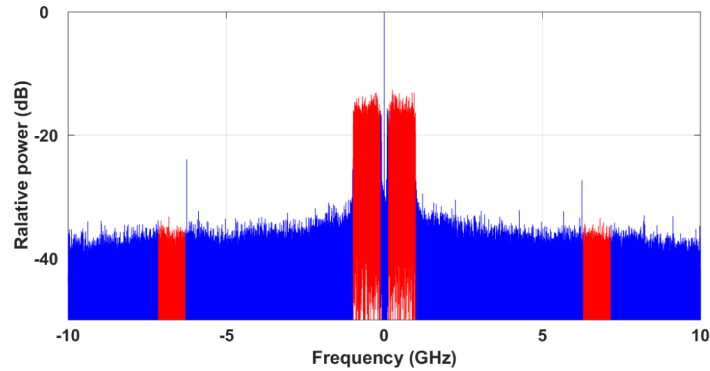


Fig. 10. The SNR measurement method. The noise level is estimated from the pure noise region near the signal by assuming that the noise level is uniform in a wide range.

First, we assess the validity of the SBS amplification with different gains for OFDM signal. We fix the signal bandwidth to 2 GHz and set the guard band between each two signal bands to 500 MHz. 2.2-GHz gain filters are used for amplification. The SNR-BER curves for the QPSK format are presented in Fig. 11(a) while the 16-QAM case in Fig. 11(b). Different constellation diagrams are also given in the insets. After being amplified by the SBS gain filter with 25-dB gain, the SNR penalties are only ~ 0.2 dB and ~ 1.7 dB at a BER of 10^{-3} for QPSK and 16-QAM respectively. For 16-QAM, larger penalty has been observed when the SNR is high in large gain cases because of the large SBS-ASE noise. The result has proved that the SBS gain induced penalty is not significant especially when the signal format is QPSK. It has also validated the feasibility of the proposed rectangular SBS gain filter in the OFDM system.

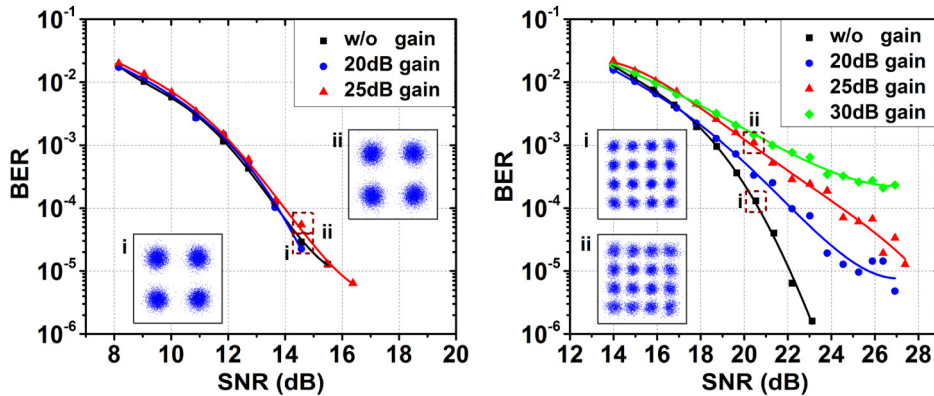


Fig. 11. BER-SNR performance of (a) QPSK (b) 16-QAM format OFDM signal, only the central band being amplified.

Then the performance of the full add and drop function is measured, i.e. the dropped de-correlated single band of one branch is inserted between the two remaining side bands of the other branch. The signal is still set to 2 GHz with 500 or 300 MHz guard bands amplified or absorbed by a 2.2 GHz gain or loss filter. The filter induced penalty here is twofold: the Brillouin-ASE and the crosstalk from the remains of the absorbed central band. We study

these two factors separately. First we fix the crosstalk and change the Brillouin gain. The SBS loss is ~ 23 dB corresponding to a pump power of 24 dBm. Ensuring the added central band and two sidebands with the same power, the 23-dB SBS loss corresponds to 23-dB in-band crosstalk of the central band. The BER performances with 20, 25 and 30 dB amplification are shown in Fig. 12. For QPSK-format signal, the SNR-BER curves indicate that penalty induced by the add and drop function is ~ 0.7 dB, no matter what the Brillouin gain is. For 16-QAM signal, the penalties are increased with the increase of the SBS gain. Considering the low tolerance of the noise and crosstalk, the performance of the 16-QAM is also acceptable.

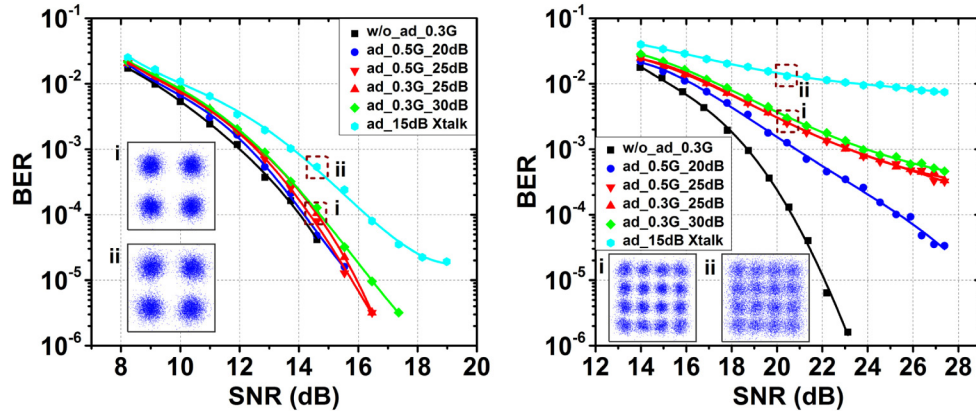


Fig. 12. BER-SNR performance of (a) QPSK (b) 16-QAM format OFDM signal with the full add and drop functions. ad: add and drop. 0.5G/0.3G: the bandwidth of the guard band. 30/25/20 dB: the SBS gain value.

Then we reduce the SBS loss from ~ 23 dB to ~ 15 dB. Thus the residual central band induces more severe crosstalk to the added central band. The guard band is set to 500 MHz. As shown in Fig. 12, the penalty for QPSK signal at BER of 10^{-3} is increased to ~ 1.8 dB at BER of 10^{-3} while the BER performance is dramatically degraded for 16-QAM. This is reasonable because the constellation points of 16-QAM format signal are closer than QPSK and are more sensitive to the noise as well as crosstalk. Since the SBS gain corresponds to the in-band crosstalk of the two side OFDM-bands, ~ 25 -dB SBS gain and loss is the basic requirements for 16-QAM format [21]. While for QPSK, the requirements are far less demanding.

Meanwhile, we also evaluate the relation between the guard band and the performance. Figure 12 shows that when the guard band is reduced from 500 MHz to 300 MHz, all the performance differences are negligible benefiting from the precise filtering technique. Thanks to the sharp rectangular response of the SBS filter, it is even possible to narrow the guard band as small as 100 MHz, but due to the limitation from the laser stability, we only set the minimum guard band to 300 MHz.

5. Conclusion

We have implemented an ultra-selective ROADMs structure and demonstrated spectral processing for MB-OFDM signal with 2-GHz granularity and 300-MHz guard band employing flexible rectangular optical filters based on SBS in optical fiber. Steep-edged flat-topped filters with tunable bandwidth from 100 MHz to 3 GHz have been realized using an optical comb as the pump. The filter passband flatness is controlled to ~ 1 dB utilizing feedback pump control with coherent detection directly using OFDM signals. Based on this rectangular filter, we demonstrate the separation and aggregation of a 3-band OFDM signal in both QPSK and 16-QAM formats. Thanks to the steep edges of the proposed filter, the guard band can be set as small as 300-MHz without any obvious extra penalty. For QPSK format

signal, the filter induced total penalty is only ~ 0.7 dB benefiting from the flat passband and smooth phase response. For 16-QAM format signal, the ROADM performance is also acceptable considering the low tolerance of the noise and crosstalk. Meanwhile, the flexibility of the OFDM is taken to the extreme with the help of the filter bandwidth flexibility. The experimental results validate the SBS-based ROADM structure and prove the feasibility of both SBS amplification and absorption in OFDM transmission and networks.

Acknowledgments

This work is supported by National Basic Research Program of China (2012CB315602), National Natural Science Foundation of China (61322507 and 61132004), Program of Excellent PhD in China (201155) and “Futur et Ruptures” program from Institut Mines Telecom in France.